Monthly Notices
of the
ROYAL ASTRONOMICAL SOCIETY

MNRAS **488,** 2644–2649 (2019)
Advance Access publication 2019 July 10

doi:10.1093/mnras/stz1892

Constraints on the formation of brown dwarfs by turbulent compression

Torsten Stamer ★ and Shu-ichiro Inutsuka ★

Nagoya University, Furo-cho, Chikusa-ku, 464-8602 Nagoya, Japan

Accepted 2019 July 5. Received 2019 July 2; in original form 2019 June 2

ABSTRACT

We perform radiation hydrodynamical simulations in spherical symmetry in order to investigate the formation of very low mass objects, i.e. brown dwarfs, by external compression. According to the Jeans stability criterion, a very low mass molecular cloud core must reach a very high density in order to become gravitationally unstable. One possibility to create such a high density is the compression by turbulent flows within the larger molecular cloud. Using our self-developed radiation hydrodynamics code, we aim to test the validity of this scenario, and to constrain the strength of the turbulence that is needed. We find that the probability for sufficiently strong and long-lived turbulence is very low under typical conditions even when using very optimistic assumptions, and therefore conclude that turbulent compression is unlikely to be the dominant mechanism for creating brown dwarfs. We also investigate the properties of objects formed by this turbulent compression process. Specifically, we compare the lifetime of the first core stage for the cases with and without external compression. We confirm our previous findings that the first core lifetime increases by about an order of magnitude at the extremely low-mass end, but this increase is somewhat less dramatic and occurs at even lower masses than in our previous work, in which no external compression was present.

Key words: brown dwarfs – stars: formation – stars: pre-main-sequence.

1 INTRODUCTION

Star formation takes place in the cold and dense regions of the interstellar medium known as molecular clouds, specifically within filaments in these clouds. These filaments are elongated regions of higher gas density, with a characteristic width of 0.1 pc and lengths of a few to tens of pc. Inutsuka & Miyama (1992, 1997) showed that such filaments become gravitationally unstable when their line mass (i.e. mass per length) exceeds a critical value of $M_{\rm line,crit} \approx 16\,{\rm M}_\odot\,{\rm pc}^{-1} \times (T_{\rm gas}/10\,{\rm K})$. Observations, e.g. André et al. (2010), show that pre- and protostellar cores are found almost exclusively in regions where this stability criterion is violated. Intersections between different filaments may create the regions most conducive to star formation, and especially star cluster formation, due to localized higher density (Myers 2009, 2011; Schneider et al. 2012). Furthermore, Inutsuka & Miyama (1992, 1997) found that filaments are unstable to longitudinal perturbations, which grow and cause the radially collapsing filament to fragment into a number of pre-stellar cores, which then continue to collapse and ultimately form protostars.

This description of star formation applies to low-mass stars such as the Sun. However, our focus in this work is brown dwarfs, which are substellar objects with masses between about 1 and 8 per cent of the solar mass. They are similar to very low-mass stars in many ways, and might be formed in the same way (e.g. Chabrier et al. 2014). The difference between brown dwarfs and stars is that brown dwarfs have such low mass that their core temperature never becomes hot enough to sustain hydrogen fusion (although deuterium fusion can occur). This means that brown dwarfs lack an internal energy source; after their formation they simply cool down over time, so unlike in the case of stars there is a direct relationship between age and temperature. Observations suggest that the number of brown dwarfs is comparable to that of low-mass stars, but their formation has puzzled researchers for some time. The problem is easily understood by considering the Jeans stability criterion: It is believed that star formation takes place when a molecular cloud core exceeds its Jeans mass $M_{\rm J} = c_{\rm s}^3 G^{-3/2} \rho^{-1/2}$. Given that the typical temperature in molecular clouds is 10 K, and assuming that the mass of the star that is formed ($M_\star$) is similar to the Jeans mass, we can calculate the density that the original cloud core must have in order to be unstable:

$$\rho = \left(\frac{c_{\rm s}^3 G^{-3/2}}{M_\star} \right)^2 . \quad (1)$$

For $M_\star = {\rm M}_\odot$, this evaluates to roughly 10^4 cm^{-3}, which is in line with typical observations of high-density star-forming regions. But the required number density increases to 10^6 cm^{-3} for $M_\star = 0.1\,{\rm M}_\odot$ (slightly above the brown dwarf/star boundary) and 10^8 cm^{-3}

* E-mail: tostamer@gmail.com (TS); inutsuka@nagoya-u.jp (S-iI)

for $M_\star = 0.01$ $M_\odot$ (a low-mass brown dwarf). This far exceeds the observed densities in molecular clouds. Hence the question arises: Which mechanism is responsible for creating such extremely high-density regions as are necessary for brown dwarf formation? Broadly speaking, there are two possibilities.

(i) The same mechanism that creates 'normal' pre-stellar cores also produces pre-brown dwarf cores.
(ii) One or more other mechanisms are important, and possibly even dominant, in brown dwarf formation.

The issue is complicated by the difficulty of observing pre- or proto-brown dwarfs, although a few likely candidates are known (Barrado et al. 2009; André et al. 2010; Palau et al. 2014; Tokuda et al. 2019). The core mass function and initial mass function in the very low mass regime are poorly known, so it is still unclear whether the core mass function (CMF) and initial mass function (IMF) are universal (i.e. apply to all mass ranges from brown dwarfs to massive stars). The former case would imply that brown dwarf formation is simply a scaled down version of low-mass star formation; the latter would imply that alternative mechanisms are at play.

A number of such alternative scenarios have been proposed to explain brown dwarf formation. One possibility is the gravitational fragmentation of protostellar discs (Stamatellos, Hubber & Whitworth 2007; Stamatellos & Whitworth 2008). While it is known that discs can become unstable and create smaller mass objects such as brown dwarfs or gaseous planets even in non-ideal magnetohydrodynamical simulations (Inutsuka et al. 2010; Machida, Inutsuka & Matsumoto 2011), it is unclear whether sufficiently massive accretion discs can commonly form. Given the comparable number of brown dwarfs and low-mass stars, on average about one brown dwarf should form in the disc of every low-mass star, which at this point seems very unlikely.

Another possibility is so-called 'competitive accretion and ejection', investigated by e.g. Reipurth & Clarke (2001) and Bate (2009): in this scenario, a higher mass pre-stellar core results in the formation of multiple protostars. Gravitational interactions between these can then cause some to be ejected from the parent cloud, so that they lose their accretion reservoir and can no longer grow in mass. Originally, it was believed that this scenario should cause a larger-than-observed velocity dispersion for brown dwarfs, but later numerical simulations such as Bate (2009) showed that this was not the case and that the predictions agree well with observations (e.g. Joergens 2006; Kurosawa, Harries & Littlefair 2006). Therefore, this scenario remains one of the main contenders to explain brown dwarf formation.

Furthermore, Whitworth & Zinnecker (2004) have suggested that a brown dwarf can be created when a core that is originally more massive has part of its material eroded due to ionizing radiation from nearby OB stars (photoerosion). However, there are no observations showing an excess of brown dwarfs in the vicinity of massive stars, and brown dwarf formation is certainly possible without any massive stars nearby, so this mechanism does not appear to be dominant.

In contrast to the filament paradigm we described in the beginning, which is dominated by gravity, in works like Padoan et al. (2001), Padoan & Nordlund (2002), and Tilley & Pudritz (2004) the formation of pre-stellar cores and pre-brown dwarfs is described as a process dominated by turbulence. In this paradigm, stars form wherever the collision of turbulent flows creates a sufficiently dense (i.e. Jeans unstable) condensation. However, these calculations are isothermal, so they do not consider the stabilizing effect of the temperature/pressure increase in the transient post-shock regions. This is especially problematic for very low mass (brown dwarf) cores, which are inherently more difficult to collapse due to the extreme densities required. Lomax, Whitworth & Hubber (2016) used smoothed particle hydrodynamics (SPH) calculations of colliding flows to simulate brown dwarf formation in this way, and they found that an unrealistically high degree of convergence of the initial flow field is required in order to create a gravitationally bound object.

In this paper, we adopt a different model to tackle the problem, using the radiation hydrodynamics code described in our previous paper (Stamer & Inutsuka 2018a). Instead of colliding flows, we begin with a static cloud core and apply a strong external pressure to its outer boundary. If this pressure is strong enough, it can cause an otherwise stable cloud core to collapse and form a brown dwarf. Our approach does not require any assumption about the flow field, and it allows us to estimate the scale of turbulence necessary to form brown dwarfs by turbulent compression. Our aim is to constrain the conditions under which this formation mechanism can operate: What are the necessary cloud densities and how strong does the turbulence need to be? Are these conditions commonly achievable in nature? In addition, what differences arise in the protostellar collapse process if an object is formed as a result of external compression?

As a final note, it should be mentioned that the various theories for brown dwarf formation are not mutually exclusive. It is likely that all of them can and do occur in nature, but it is unclear how important they are relative to each other. For instance, in a study of brown dwarfs orbiting solar-type stars, Ma & Ge (2014) find evidence of two distinct populations. Based on different eccentricity distributions, they suggest that objects below $\approx 43 M_J$ in their sample have mostly formed from disc instabilities, making them similar to giant planets. On the other hand, the heavier objects are the result of molecular cloud core collapse, meaning these systems are better characterized as binaries. More detailed observations, as well as numerical simulations, are necessary to better estimate the contribution of the various possible formation channels.

2 SIMULATION SET-UP

2.1 Overall method

The simulation program is the same as in our previous paper (Stamer & Inutsuka 2018b, hereafter Paper 1). It uses a hydrodynamics module based on Colella & Woodward (1984) and includes self-gravity and a non-ideal equation of state provided by Tomida et al. (2013) and Tomida, Okuzumi & Machida (2015), which includes the effect of hydrogen dissociation. Radiation transfer is treated with our frequency-dependent spherically symmetric scheme developed in Stamer & Inutsuka (2018a). Please refer to this paper and Paper 1 for more details on the radiative transfer scheme, opacities, and radiative boundary conditions.

2.2 Initial conditions

We envision an isothermal brown dwarf mass cloud core that is initially in hydrostatic equilibrium and stable to gravitational collapse, i.e. a subcritical Bonnor–Ebert sphere (Ebert 1955; Bonnor 1956). Because the larger molecular cloud is highly turbulent, there will be regions of higher pressure within it. If the cloud core has formed within such a region of high turbulent pressure, it will be compressed further, and if this compression is sufficiently strong, the core may be destabilized and collapse. We model this process

by adding an external pressure at the outer boundary of our system:

$$P_{\rm ext} = P_{\rm ext,init}\, {\rm e}^{-\frac{t}{t_{\rm D}}}, \tag{2}$$

where $t_{\rm D}$ is the time-scale at which this external pressure decays. This decay represents the fact that the turbulent fluctuations in the cloud only exist for a limited time. Our simulation has the following parameters:

(i) $n_{\rm C}$ (central number density);
(ii) $R_{\rm O}$ (initial cloud core radius);
(iii) $P_{\rm ext,\,init}$ (initial external pressure);
(iv) $t_{\rm D}$ (time-scale for the external pressure to decay).

Hydrostatic equilibrium for a self-gravitating isothermal sphere can be described by the following equation:

$$\frac{{\rm d}P}{{\rm d}r} = -G\frac{M(r)}{r^2}, \tag{3}$$

where $M(r)$ is the enclosed mass at radius r. We assume a constant temperature of 10 K and set up the system by fixing $n_{\rm C}$ and $R_{\rm O}$ and numerically integrating this equation outward from the centre. The total mass is then determined, as is $P_{\rm O}$, the pressure at the outer boundary. The external pressure is then added on top of $P_{\rm O}$. An important derived parameter is the Bonnor–Ebert mass $M_{\rm BE} = 1.18 c_{\rm s}^4 P_{\rm O}^{-1/2} G^{-3/2}$, which is the critical mass above which the core would be unstable to gravitational collapse even without any external pressure. Its role is similar to that of the Jeans mass $M_{\rm J}$ in the case of initially homogeneous density. For all the calculations in Section 3.1, $M < M_{\rm BE}$, and for all those in Section 3.2, $M < M_{\rm J}$. This means that without an external pressure, none of our simulated cores would collapse.

3 RESULTS

3.1 Conditions for collapse

We perform a number of simulations while varying the parameters described in the previous section. The presence of a large external pressure causes a shock wave that moves from the outer boundary towards the centre in the form of a density and temperature spike. After this shock wave reaches the centre and is reflected there, two possibilities exist. Either the compression is sufficiently strong to destabilize the system, in which case the collapse proceeds to form a first hydrostatic core. Otherwise, the system only oscillates but does not collapse. Fig. 1 shows which is the case for different combinations of parameters for a 0.06 $M_\odot$ core. We find the following results.

(i) Larger external pressures and longer decay times are more favourable in order to trigger a collapse, as should be expected.

(ii) Set-ups with higher central density appear to be more resistant to collapse. This may seem unintuitive at first, but it becomes clear when one considers the thermal pressure. For example, in the case of $n_{\rm C} = 10^6$ cm^{-3} and $T = 10$ K, the internal pressure is $10^7 k_{\rm B}$ dyn cm^{-2}. It is obvious that an additional external pressure that is much lower than this will have no significant effect on the overall evolution, no matter for how long it acts. Thus the ratio between the internal and external pressure is important.

(iii) With the previous consideration, we see that the higher density cores, whose ratio of M to $M_{\rm BE}$ is larger, are actually more unstable. For example, in the case of $n_{\rm C} = 10^4$ cm^{-3}, an external pressure one or even two orders of magnitude larger than the internal pressure still fails to cause a collapse if the decay time is short. On the other hand, for $n_{\rm C} = 10^6$ cm^{-3}, an additional external pressure equal to the internal pressure can be enough to cause a collapse, provided it acts for a long enough time.

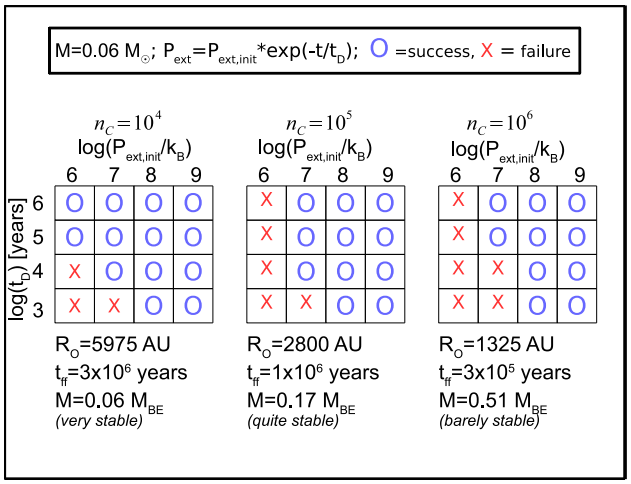

Figure 1. Forming brown dwarfs by turbulent compression. The initial temperature is 10 K and the total core mass is 0.06 $M_\odot$. The three boxes correspond to three different central densities. Within each box, different columns represent different values of the initial external pressure, and different rows represent different values of the decay time-scale. For each box, the initial core radius, the free-fall time, and the mass in units of the Bonnor–Ebert mass are given. A blue circle for a combination of parameters signals that a collapse occurred in that calculation, i.e. a proto-brown dwarf was formed. Red X symbols mean that in this calculation, the core only oscillated without ever collapsing.

In summary, the qualitative behaviour of the above results can be understood. Next, we wish to interpret them quantitatively. Assuming typical molecular cloud conditions, how common are turbulent fluctuations that are both sufficiently strong and exist for a sufficiently long time? We give a rough estimate with the following approach.

First, we assume the lifetime of turbulent fluctuations to be similar to the crossing time of the turbulent motion:

$$t_{\rm c} = \frac{R}{v_{\rm turb}} = \frac{R}{\mathcal{M} c_{\rm s}}, \tag{4}$$

where R is the spatial size of the fluctuation (i.e. the radius of the cloud core) and $v_{\rm turb}$ is the typical turbulent velocity, which can be derived from the Mach number $\mathcal{M}$ and the sound speed $c_{\rm s}$, which we take to be 0.2 km s^{-1}. Our simulations tell us that in order to form a brown dwarf, the fluctuation needs to exist for a certain minimum time $t_{\rm D}$. For a given core radius, this results in an upper limit on the Mach number $\mathcal{M}_{\rm max} = R/(t_{\rm D} c_{\rm s})$, because turbulence that is too strong will 'blow over' too quickly for the core to become destabilized.

On the other hand, stronger turbulence is helpful for brown dwarf formation because it makes it more likely to create very high pressure regions. In the second step, we use the previously derived upper limit of the Mach number to calculate the probability of turbulent fluctuations whose pressure is at least as strong as the pressure required according to our simulation results. The probability density function for the density (and therefore, under isothermal conditions, for the pressure) in supersonic turbulence in molecular clouds is generally assumed to have a lognormal shape (Vazquez-Semadeni 1994; Kritsuk et al. 2007; Hennebelle & Chabrier 2008;

Table 1. Probabilities P to achieve the pressure fluctuations corresponding to the runs shown in Fig. 1, for the most easily achievable case $n_C = 10^4$ cm^{-3}. The probabilities were calculated using the upper limit on the Mach number as described in the text of Section 3.1. The runs with $t_D = 10^6$ yr are not shown since they would require a subsonic Mach number and their probabilities are near 0.

$\log(P_{\rm ext,\,init})$ (k_B dyn cm^{-2})	$\log(t_D)$ (yr)	$\mathcal{M}_{\rm max}$	P	Comment
6	3	141	6×10^{-3}	No collapse; $\mathcal{M}_{\rm max}$ unrealistic
6	4	14.1	6×10^{-3}	No collapse
6	5	1.4	3×10^{-7}	
7	3	141	2×10^{-3}	No collapse; $\mathcal{M}_{\rm max}$ unrealistic
7	4	14.1	1×10^{-3}	Most easily achievable combination that actually collapsed
7	5	1.4	2×10^{-11}	
8	3	141	8×10^{-4}	$\mathcal{M}_{\rm max}$ unrealistic
8	4	14.1	2×10^{-4}	
8	5	1.4	2×10^{-16}	
9	3	141	2×10^{-4}	$\mathcal{M}_{\rm max}$ unrealistic
9	4	14.1	3×10^{-5}	
9	5	1.4	1×10^{-22}	

Federrath & Klessen 2012), specifically

$$\mathrm{PDF}(\delta) = \frac{1}{\sqrt{2\pi\sigma_0^2}} \exp\left(-\frac{(\delta-\overline{\delta})^2}{2\sigma_0^2}\right), \quad (5)$$

where $\delta = \log(\rho/\overline{\rho})$, with $\overline{\rho}$ the average cloud density, $\overline{\delta} = -\sigma_0^2/2$, and $\sigma_0^2 = \ln(1 + b\mathcal{M}^2)$. The parameter b is empirically determined to be around 0.25, and a typical value for the average density in molecular clouds is 10^2 cm^{-3}, which we shall adopt here. The average pressure is therefore $10^3 k_B$ dyn cm^{-2}. By inserting our previously derived upper limit on the Mach number in equation (5), we can calculate the probability for a fluctuation whose density/pressure enhancement is larger than some value δ_c:

$$\delta_c = \int_{\delta_c}^{\infty} \mathrm{PDF}(\delta)\,\mathrm{d}\delta. \quad (6)$$

For example, when calculating the probability of achieving a turbulent pressure above $10^6 k_B$ dyn cm^{-2}, we would choose $\delta_c = 3$. To summarize, equation (6) allows us to estimate the probability to find, at any point in the cloud at any moment in time, a turbulent fluctuation that is strong enough that it could create a brown dwarf, under the assumption that the Mach number is equal to the upper limit imposed by the time-scale constraint.

Among our simulation runs, the easiest conditions to achieve are those with the lowest density, since these cores are larger (allowing for a larger Mach number) and they require only a comparatively weak pressure enhancement. [1]

The results are shown in Table 1. The most easily achievable combination that successfully forms a brown dwarf only has a probability of 1×10^{-3}. For the most optimistic estimation, we could assume that the combination of $\log(P_{\rm ext,\,init}) = 6$ and $\log(t_D) = 4$, which failed to produce a brown dwarf, was actually very close to collapsing. Even such a fluctuation is difficult to achieve however, as the probability is only 6×10^{-3} with $\mathcal{M}$ =14. Recall also that all of these calculations are based on a 0.06 $M_\odot$ object, which is relatively heavy by brown dwarf standards. For smaller masses, the odds would get even worse since the core radius, and therefore the upper limit on the Mach number, would be reduced further. We must therefore conclude that the formation of brown dwarfs, and especially low-mass brown dwarfs, by this process is not very effective, since the necessary conditions can only be achieved very rarely. Of course, our estimation is very rough, and the details of the turbulence in molecular clouds are still poorly understood. A better estimation of the likelihood of this scenario would require more observations to constrain the strength and time-scale of the turbulent fluctuations.

[1] We also attempted to form brown dwarfs from an even lower initial density of 10^3 cm^{-3}, but this did not improve the chances any more, since the required external pressures and time-scales were no smaller than in the case of 10^4 cm^{-3}.

3.2 Lifetime of the first core

We performed additional simulation runs in which we analysed the collapse process in more detail. For simplification, we begin with a homogeneous density, and we no longer let the external pressure decay, i.e. $t_D = \infty$. This is because at this point, we are not concerned with whether or not a core collapses under realistic conditions. Instead, we investigate the process for cases in which an external pressure did successfully cause a collapse. We originally chose 11 different masses between 0.007 and 0.1 $M_\odot$ (the same ones as the runs labelled 'A0' through 'A10' in Paper 1). The initial number densities are 10^4, 10^5, and 10^6 cm^{-3}, and the external pressure is either equal to or one order of magnitude larger than the initial thermal pressure (weak or strong compression). In the highest density runs with strong compression, a collapse still occurs even at the lower end of our initial mass range. To find the minimum mass needed for a collapse at this density and external pressure, we performed a further six runs with masses running from 0.006 down to 0.001 $M_\odot$. This makes for a grand total of 72 runs, 30 of which collapsed to form a protostar. These are listed in Table 2.

In the weak compression case, the only initial conditions that lead to a collapse are $n = 10^6$ cm^{-3} and a mass of 0.058 $M_\odot$ or more. If the compression is strong, all of the highest density runs down to 0.005 $M_\odot$ successfully form a brown dwarf, while for $n = 10^5$ cm^{-3}, only those with a mass of 0.012 $M_\odot$ or more do, and for $n = 10^4$ cm^{-3}, this minimum mass rises to 0.035 $M_\odot$. This again indicates that a collapse becomes easier to trigger the more dense and massive the core is, as should be expected. More powerful compression and higher initial density allow for the formation of lower mass objects.

We are also interested in the lifetime of the first core, since it relates to our results in Paper 1. There we found that for a total mass below about 0.02 $M_\odot$, the first core can exist much longer

Table 2. Overview of our simulation runs. The values are, from left to right: run label, logarithm of the initial number density, total mass, logarithm of the external pressure, initial radius, free-fall time, ratio of mass to Jeans mass, time until first core formation, and first core lifetime.

Label	log n (cm^{-3})	M (M$_\odot$)	log $P_{\rm ext}$ ($k_{\rm B}$ dyn cm^{-2})	R (au)	$t_{\rm ff}$ (yr)	$M/M_{\rm J}$	$t_{\rm FC}$ (yr)	$\tau_{\rm FC}$ (yr)
4356	4	3.5e-02	6	5.0e + 03	3.3e + 05	3.0e-02	4.2e + 04	1.1e + 03
4586	4	5.8e-02	6	5.9e + 03	3.3e + 05	6.0e-02	4.4e + 04	1.1e + 03
4716	4	7.1e-02	6	6.3e + 03	3.3e + 05	7.0e-02	4.6e + 04	1.3e + 03
4856	4	8.5e-02	6	6.7e + 03	3.3e + 05	8.0e-02	4.9e + 04	1.4e + 03
41006	4	1.0e-01	6	7.0e + 03	3.3e + 05	1.0e-01	5.1e + 04	1.6e + 03
5127	5	1.2e-02	7	1.6e + 03	1.0e + 05	4.0e-02	1.5e + 04	1.9e + 03
5157	5	1.5e-02	7	1.7e + 03	1.0e + 05	5.0e-02	1.5e + 04	1.5e + 03
5217	5	2.1e-02	7	1.9e + 03	1.0e + 05	7.0e-02	1.5e + 04	1.4e + 03
5357	5	3.5e-02	7	2.3e + 03	1.0e + 05	1.1e-01	1.7e + 04	1.3e + 03
5587	5	5.8e-02	7	2.7e + 03	1.0e + 05	1.8e-01	1.9e + 04	1.2e + 03
5717	5	7.1e-02	7	2.9e + 03	1.0e + 05	2.2e-01	2.1e + 04	1.2e + 03
5857	5	8.5e-02	7	3.1e + 03	1.0e + 05	2.7e-01	2.2e + 04	1.1e + 03
51007	5	1.0e-01	7	3.3e + 03	1.0e + 05	3.1e-01	2.2e + 04	2.1e + 03
658	6	5.0e-03	8	5.6e + 02	3.3e + 04	5.0e-02	5.9e + 03	8.9e + 03
668	6	6.0e-03	8	5.9e + 02	3.3e + 04	6.0e-02	5.4e + 03	4.0e + 03
678	6	7.0e-03	8	6.2e + 02	3.3e + 04	7.0e-02	5.4e + 03	2.5e + 03
688	6	8.0e-03	8	6.5e + 02	3.3e + 04	8.0e-02	5.4e + 03	1.8e + 03
6108	6	1.0e-02	8	7.0e + 02	3.3e + 04	1.0e-01	5.6e + 03	1.4e + 03
6128	6	1.2e-02	8	7.5e + 02	3.3e + 04	1.2e-01	5.8e + 03	1.3e + 03
6158	6	1.5e-02	8	8.0e + 02	3.3e + 04	1.5e-01	6.1e + 03	1.1e + 03
6218	6	2.1e-02	8	9.0e + 02	3.3e + 04	2.1e-01	6.1e + 03	1.5e + 03
6358	6	3.5e-02	8	1.1e + 03	3.3e + 04	3.5e-01	7.1e + 03	1.2e + 03
6587	6	5.8e-02	7	1.3e + 03	3.3e + 04	5.7e-01	2.9e + 04	6.4e + 02
6588	6	5.8e-02	8	1.3e + 03	3.3e + 04	5.7e-01	8.4e + 03	9.6e + 02
6717	6	7.1e-02	7	1.4e + 03	3.3e + 04	7.0e-01	2.6e + 04	6.4e + 02
6718	6	7.1e-02	8	1.4e + 03	3.3e + 04	7.0e-01	9.0e + 03	8.9e + 02
6857	6	8.5e-02	7	1.4e + 03	3.3e + 04	8.4e-01	2.5e + 04	6.1e + 02
6858	6	8.5e-02	8	1.4e + 03	3.3e + 04	8.4e-01	9.5e + 03	8.4e + 02
61007	6	1.0e-01	7	1.5e + 03	3.3e + 04	9.9e-01	2.5e + 04	6.2e + 02
61008	6	1.0e-01	8	1.5e + 03	3.3e + 04	9.9e-01	1.0e + 04	7.7e + 02

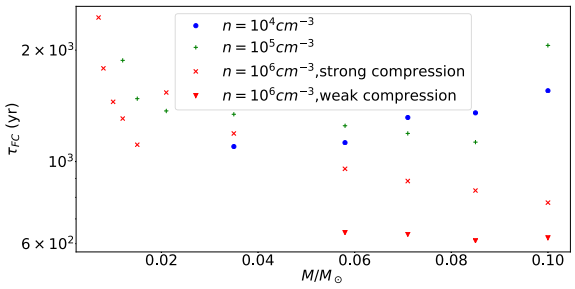

Figure 2. First core lifetime plotted against total mass. Different subsets of runs use different symbols.

than otherwise. This happens because in such low-mass cases, the envelope that surrounds the core is depleted before the temperature reaches 2000 K and triggers the second collapse. As a result, the first core lifetime, which is on the order of 1000 yr and only weakly dependent on the total mass if $M > 0.02\,{\rm M}_\odot$, begins to rise dramatically and can reach more than 10 000 yr for masses below this threshold, in agreement with previous results by Tomida et al. (2010).

Our results for the external compression case are shown in Fig. 2, which illustrates the first core lifetime's dependence on the total mass. As in Paper 1, a drastic increase by about an order of magnitude can be observed for very low masses, though this is only visible in the highest density runs since they are the only ones that collapsed at these low masses. Significantly, this increase occurs at even lower masses than in Paper 1, with a threshold near $0.01\,{\rm M}_\odot$. For comparison, at $M = 0.007\,{\rm M}_\odot$ the lifetime is 2500 yr in this work, but 14 900 yr in Paper 1. Note that in the previous paper, the collapse is triggered because the initial conditions are Jeans unstable. In this work, however, the initial conditions are Jeans stable, and the collapse is induced by the external pressure.

The likely explanation for the shorter first core lifetimes is that the presence of an external pressure causes a more vigorous initial collapse. This is also evident when looking at $t_{\rm FC}$, the time until first core formation: without an external pressure, it is slightly longer than the free-fall time. However, in our results here, $t_{\rm FC} < t_{\rm ff}$ for the weak compression cases, and $t_{\rm FC} << t_{\rm ff}$ for strong compression (see Table 2), so the whole process happens on a much faster time-scale. The first core forms once the thermal pressure balances the sum of the ram pressure of the infalling gas and the external pressure (although the latter is negligible by that point). With a more vigorous collapse, the ram pressure is larger, so the first core already starts out with a higher density and temperature. The accretion rate is also larger, and as a result, reaching the temperature necessary for the second collapse takes less time.

We also find a difference in the first core lifetimes for the weak and strong compression cases. The four combinations of density and mass that lead to a collapse in both cases have first core lifetimes around 600 yr for weak and 800–900 yr for strong compression, i.e. stronger external compression leads to a slightly longer first core stage. This appears contradictory since we previously stated that a more vigorous collapse should lead to a shorter first core lifetime. The explanation is related to the initial shock wave caused by the

external pressure: Since the system is still optically thin in the early stages, the temperature spike caused by the shock leads to radiative losses and a decrease in the system's entropy, the magnitude of which depends on the strength of the shock. Later in the first core stage, lower entropy means that a higher density is required to achieve the same temperature. Since the first core phase lasts until the temperature reaches 2000 K, this effect causes it to last longer. In practice, in the weak compression runs the central temperature reaches 2000 K when the density is around 5×10^{-8} g cm^{-3}, while in the strong compression runs, it only does so at about 9×10^{-8} g cm^{-3}.

In summary, the presence of an external pressure results in a more vigorous collapse, which reduces the first core lifetime. However, it also results in more radiative losses in the early stage, so even stronger external pressures ultimately cause the lifetime to increase again.

Finally, it should be mentioned that our simulation, being spherically symmetric, includes neither rotation nor magnetic fields. Investigating the impact of these effects on the first core lifetime requires more sophisticated models (see e.g. Bate 2011 for a rotating core and Commerçon et al. 2010; Tomida et al. 2013; Bate, Tricco & Price 2014; Tsukamoto et al. 2015 for magnetohydrodynamical calculations). Reviews can be found in Inutsuka (2012) and Tsukamoto (2016).

4 SUMMARY

We performed spherically symmetric radiation hydrodynamics simulations of protostellar collapse. First, we investigated the stability of low-mass molecular cloud cores subjected to an external pressure. This external pressure is intended to simulate the cloud core being embedded in a turbulent high-pressure region within the molecular cloud. Our results showed that, even under optimistic assumptions, it is very hard to cause brown dwarf mass cloud cores to collapse under typical molecular cloud conditions, because the requirements on the strength and longevity of the turbulent fluctuations are quite strict. However, in order to better estimate the efficiency of the turbulent compression mechanism, more observations of the actual turbulence patterns in molecular clouds are needed to form a better understanding.

In the second part of our results, we analysed the properties of brown dwarfs formed by turbulent compression, particularly the lifetime of the first core. In our previous paper, we found that the first core, which typically lives for about 10^3 yr, can exist for more than 10^4 yr for objects below about 0.02 $M_\odot$ as a result of envelope depletion. Those results were obtained without any external compression; instead, the initial cloud cores were so extremely dense that they were Jeans unstable from the onset. Despite this difference, our results in this paper show a similar pattern in which the first core lifetime increases dramatically below a certain mass, but in this case the threshold is closer to 0.01 $M_\odot$ and the increase is less extreme. We conclude that this is due to the initial collapse being more vigorous in the presence of an external pressure, although there is also a competing opposite effect in which an even larger external pressure actually increases the first core lifetime by causing a larger loss of entropy in the early stage of the collapse. However, since the conditions for successful turbulent compression are extremely limited and not usually expected to be achieved, it should be difficult to observe such short-lived first cores created by turbulent compression in actual molecular clouds.

REFERENCES

André P., Men'shchikov A., Bontemps S., Könyves V., Motte F., Schneider N., Di Francesco J., 2010, A&A, 518, L102
Barrado D., Morales-Calderón M., Palau A., Bayo A., de Gregorio-Monsalvo I., Eiroa C., Schmidtobreick L., 2009, A&A, 508, 859
Bate M. R., 2009, MNRAS, 392, 590
Bate M. R., 2011, MNRAS, 417, 2036
Bate M. R., Tricco T. S., Price D. J., 2014, MNRAS, 437, 77
Bonnor W. B., 1956, MNRAS, 116, 351
Chabrier G., Johansen A., Janson M., Rafikov R., 2014, in Beuther H., Klessen R. S., Dullemond C. P., Henning T., eds, Protostars and Planets VI. Univ. Arizona Press, Tucson, AZ, p. 619
Colella P., Woodward P. R., 1984, J. Comput. Phys., 54, 174
Commerçon B., Hennebelle P., Audit E., Chabrier G., Teyssier R., 2010, A&A, 510, L3
Ebert R., 1955, Z. Astrophys., 37, 217
Federrath C., Klessen R. S., 2012, ApJ, 761, 156
Hennebelle P., Chabrier G., 2008, ApJ, 684, 395
Inutsuka S.-i., 2012, Progress Theor. Exp. Phys., 2012, 01A307
Inutsuka S.-i., Miyama S. M., 1992, ApJ, 388, 392
Inutsuka S.-i., Miyama S. M., 1997, ApJ, 480, 681
Inutsuka S.-i., Machida M. N., Matsumoto T., 2010, ApJ, 718, L58
Joergens V., 2006, A&A, 446, 1165
Kritsuk A. G., Norman M. L., Padoan P., Wagner R., 2007, ApJ, 665, 416
Kurosawa R., Harries T. J., Littlefair S. P., 2006, MNRAS, 372, 1879
Lomax O., Whitworth A. P., Hubber D. A., 2016, MNRAS, 458, 1242
Ma B., Ge J., 2014, MNRAS, 439, 2781
Machida M. N., Inutsuka S.-i., Matsumoto T., 2011, ApJ, 729, 42
Myers P. C., 2009, ApJ, 700, 1609
Myers P. C., 2011, ApJ, 735, 82
Padoan P., Nordlund Å., 2002, ApJ, 576, 870
Padoan P., Juvela M., Goodman A. A., Nordlund Å., 2001, ApJ, 553, 227
Palau A., Zapata L. A., Rodríguez L. F., Bouy H., Barrado D., Morales-Calderón M., Li D., 2014, MNRAS, 444, 833
Reipurth B., Clarke C., 2001, AJ, 122, 432
Schneider N. E. A., Csengeri T., Hennemann M., Motte F., Didelon P., Federrath C., André P., 2012, A&A, 540, L11
Stamatellos D., Whitworth A. P., 2008, MNRAS, 392, 413
Stamatellos D., Hubber D. A., Whitworth A. P., 2007, MNRAS, 382, L30
Stamer T., Inutsuka S.-i., 2018a, AJ, 155, 253
Stamer T., Inutsuka S.-i., 2018b, ApJ, 869, 179 (Paper 1)
Tilley D. A., Pudritz R. E., 2004, MNRAS, 353, 769
Tokuda K. et al., 2019, PASJ
Tomida K., Machida M. N., Saigo K., Tomisaka K., Matsumoto T., 2010, ApJ, 725, L239
Tomida K., Tomisaka K., Matsumoto T., Hori Y., Okuzumi S., Machida M. N., Saigo K., 2013, ApJ, 763, 6
Tomida K., Okuzumi S., Machida M. N., 2015, ApJ, 801, 117
Tsukamoto Y., 2016, Publ. Astron. Soc. Aust., 33, e010
Tsukamoto Y., Iwasaki K., Okuzumi S., Machida M. N., Inutsuka S.-i., 2015, MNRAS, 452, 278
Vazquez-Semadeni E., 1994, ApJ, 423, 681
Whitworth A. P., Zinnecker H., 2004, A&A, 427, 299

This paper has been typeset from a TEX/LATEX file prepared by the author.